Joint Precoding and Array Design for Broadcast in the Internet of Unmanned Aerial Vehicles

Dongsheng Zheng, Yuli Yang, Meng Ma, Wenyao Li, Bingli Jiao

Abstract—To promote energy and spectrum efficient communications in multi-antenna channels, broadcast can provide a substantial gain in system throughput. However, the hardware constraints and strong line-of-sight (LoS) limit the implementation and performance of multi-antenna broadcast in the Internet of unmanned aerial vehicles (UAVs). Based on the pseudo-Doppler principle, we propose a joint precoding and antenna array design to reduce the number of radio frequency (RF) chains required by the broadcast and free the LoS path from the inter-stream interference. The reduction of RF chains is realised by designing the precoding matrix that makes at least one of the transmit antennas have null inputs during any broadcast and, moreover, the LoS path is formed to match the obtained precoding matrix through antenna array design at the broadcasting UAV. The algorithms with low computational complexity for optimising this design are developed to minimise the transmit power within the UAV broadcast paradigms. Theoretical formulation and numerical results in the metrics of sum data rate and bit error rate substantiate the validity of our proposed design, specifically in the Internet of UAVs with strong LoS.

Index Terms—Internet of unmanned aerial vehicles (UAVs), broadcast precoding, line of sight (LoS), radio frequency (RF) chain reduction, antenna array design, pseudo-Doppler.

I. INTRODUCTION

The Internet of unmanned aerial vehicles (UAVs) has been highly developed during the past decade, which is expected to extend the coverage of terrestrial communications and offer integrated services in support of smart home and smart city [1]–[3]. In particular, UAVs are used as aerial base stations, and the non-orthogonal multiple access (NOMA) has been exploited to improve the connectivity opportunities and enhance the spectral efficiency. An efficient subchannel assignment algorithm was proposed in [4] to maximise the channel capacity for the NOMA-aided communications between an aerial base station and ground users. Moreover, the clustering-based UAV deployment and the location-based ground-user pairing were developed in [5] for a NOMA-aided network with multiple aerial base stations, to minimise the power consumption. For dense air-ground vehicle networks, an enhanced software-defined network architecture was proposed in [6], where a conceptual surveillance plane is formed as a side system for the communication links, providing local and global information to macro stations.

In addition to the resource allocation, mobility management, and stability control, which have been addressed by the aforementioned works, there are two major challenges in the Internet of UAVs: *(i)* constraints of size, weight, and power (SWAP), and *(ii)* augmented interference owing to strong line-of-sight (LoS) [7]–[9].

To achieve high spectral-efficiency while improving the quality-of-service (QoS), the deployment of multiple antennas at a UAV enables it to transmit distinct data streams to a group of peer UAVs simultaneously. Within traditional terrestrial networks, the broadcast is an efficient approach for boosting the resource utilisation efficiency while guaranteeing the QoS [10]–[12], which has been exploited in a wide range of applications [13]–[16]. In particular, precoding at block level [17]–[19] or symbol level [20]–[22] is utilised to alleviate, align or capitalize on the inter-stream interference in the broadcast. However, the SWAP constraints on UAVs impede the utilisation of multi-antenna broadcast precoding in the Internet of UAVs, mainly because the radio-frequency (RF) chains connected to multiple antennas contribute towards bigger and heavier UAVs as well as higher power consumption [23], [24]. Against this backdrop, we intend to reduce the number of RF chains in the transmitting UAV for the implementation of multi-antenna broadcast in the Internet of UAVs, which will therefore reduce the hardware complexity and power consumption of broadcasting UAVs as well as meet their SWAP constraints and increase their lifetime.

In the literature, several approaches have been introduced for the purpose of RF chain reduction in the maintenance or improvement of multi-antenna QoS. Among them, an attractive solution is spatial modulation (SM), which requires a single RF chain to increase the achievable data rate of multi-antenna systems by mapping a portion of information onto the transmit antenna (TA) index [25]–[27]. The SM concept was exploited in broadcast channels [28], [29]. In [30], a precoding scheme was conceived to divide the TAs into groups, where each group adhering to one RF chain serves a single receiver, based on SM. Hence, the number of RF chains is equal to the number of receivers. Moreover, the generalised SM was combined with block diagonalization precoding in [31] to deal with the inter-steam interference at the broadcasting transmitter, where the number of RF chains is determined by the number of data streams, i.e., equal to the total number of all receivers' antennas. Another solution to the RF chain reduction is load modulation (LM), where the information bearing signals are used to vary the input currents to antenna load impedance rather than the input voltages to power amplifier [32], [33]. The analogue implementation of the signal sets in LM arrays

TABLE I
CONTRASTING THE NOVELTY OF OUR WORK TO THE LITERATURE.

Contributions	This Work	[10]–[16]	[17]–[22]	[25]–[27],[32]–[37]	[28]–[31]
Broadcast	✓	✓	✓		✓
Precoding	✓		✓		✓
RF Chain Reduction ‡	✓			✓	✓
$N_c < U$ #	✓				
Antenna Array Design	✓				
LoS-Dominated Channels with Doppler Effect	✓				

‡ In previous works, the minimum number of RF chains is equal to the number of broadcast data streams.
# In this paper, the number of RF chains, N_c, is less than the number of broadcast data streams, U. The maximum number of RF chains is $U - 1$ in the broadcast using BPSK modulation.

reduces the need for transmit RF chains, but has to suffer from signal distortion and crosstalk between antennas, which will result in information leakage and security risks [34]. In addition to SM and LM, hybrid RF/baseband precoding is developed in millimetre wave systems with massive multi-antenna transceivers, where analogue phase shifters are used to reduce the RF chains [35]–[37]. Although the number of RF chains is less than the number of TAs, it is still limited by the number of data streams.

On the other hand, a specific attribute of physical channels in the Internet of UAVs is the dominant LoS strength of Rician fading, which exacerbates the interference inflicted in UAV communications. The performance of previous solutions to the broadcast precoding with RF chain reduction will get even worse if the LoS strength gets higher. Specifically for the SM solutions, strong LoS generates high correlation between fading channels pertaining to different TAs and, thus, results in unsuccessful detection of the information mapped onto the TA index.

Motivated by this, we propose a novel design based on the pseudo-Doppler technique, aiming to further reduce the number of RF chains in a full elimination of LoS inter-stream interference for UAV broadcast channels. The pseudo-Doppler technique was invented for direction finding by measuring the Doppler shift induced on the signal received at each element of a circular antenna array [38]–[40]. In this work, the pseudo-Doppler principle is exploited to design the antenna array for the sake of inter-stream interference cancellation. Different from previous works that rely on the broadcast channel states to design precoding matrix, we design the precoding matrix in line with the broadcast information data and, subsequently, form the LoS path to match the obtained precoding matrix through antenna array design.

More specifically, in the proposed scheme, a multi-antenna UAV broadcasts U distinct data streams by activating the maximum of $U - 1$ RF chains. Firstly, the broadcast precoding matrix is designed to leave at least one null input in the resultant signals to be radiated by the TAs of the broadcasting UAV. Then, based on the pseudo-Doppler principle, the antenna array design at the broadcasting UAV is optimised, subject to the locations of receiving UAVs, to guarantee free inter-stream interference over the resultant LoS path. The major merit of the proposed scheme is to reduce the number of RF chains required by the broadcasting UAV while eliminating the inter-stream interference. As the TAs have opportunities to keep silent during the broadcasting, the number of active RF chains will be reduced, the transmit power will be lowered, and the broadcasting UAV's lifetime will be extended. In this way, the proposed scheme will contribute to faster heat dispelling, lower hardware complexity, and smaller UAV size.

In particular, the novelty of our work is compared with related works in Table I and the main contributions of this paper are highlighted below in three aspects.

- *Principle:* Upon the pseudo-Doppler basis, a joint design of broadcast precoding and antenna array is proposed to further reduce the number of RF chains while eliminating inter-stream interference in the Internet of UAVs. The precoding matrix is formatted to leave at least one TA silent during any broadcast and the antenna array design is exploited to free the LoS path from inter-stream interference.

- *Approach:* Our joint design is implemented by the pseudo-Doppler antenna array at the broadcasting UAV, which is illustrated by the paradigms of 1-to-2 and 1-to-3 broadcast channels. The algorithms with low computational complexity for achieving the optimal antenna array design together with the broadcast precoding matrix are developed in these two paradigms, which guarantee the validity of our design in the case with strong LoS. The paradigms can be adapted to any topology changes in a straightforward way.

- *Evaluation:* To investigate the broadcast performance of our joint design with the RF chain reduction in the Internet of UAVs, its sum data rate and bit error rate (BER) are formulated in analytic expressions. Theoretical analysis and simulation results substantiate that, opposite to traditional broadcast precoding schemes, our design achieves even better performance when the LoS strength gets higher.

The remainder of this paper is organized as follows. Firstly, Section II presents the pseudo-Doppler principle and the channel model of UAV broadcast channels. Section III proposes the general principle of joint broadcast precoding and antenna array design for the RF chain reduction within the Internet

of UAVs. Section IV introduces two paradigms to further illustrate the proposed design in the scenarios of 1-to-2 and 1-to-3 UAV broadcasting. Subsequently, Section V evaluates the performance of our joint design in terms of sum data rate and BER. Finally, Section VI concludes this paper and offers an insight of future research directions.

Throughout this paper, the following mathematical notations are used: Boldface uppercase and lowercase letters denote matrices and vectors, respectively. The conjugate and the modulus operators are denoted by $(\cdot)^*$ and $|\cdot|$, respectively. The transpose, the conjugate transpose, and the Frobenius norm of a vector or a matrix are denoted by $(\cdot)^{\mathrm{T}}$, $(\cdot)^{\dagger}$, and $\|\cdot\|_F$, respectively. Besides, $\mathcal{E}_x\{\cdot\}$ denotes the expectation with respect to a random variable x.

Fig. 1. A UAV-enabled broadcast channel model. (a) 1-to-3 UAV broadcast. (b) TA deployment at the broadcasting UAV.

II. PRELIMINARIES

In this section, the pseudo-Doppler principle and the LoS-dominated model of UAV broadcast channels are introduced as preliminaries of our work.

A. Pseudo-Doppler Principle

The pseudo-Doppler principle originated in direction finding solutions, where a rapid switching between the elements of a radar's antenna array is utilised to imitate the relative movement between the target source and the radar, for causing a Doppler shift [38]. In reality, the wavefronts arriving at an antenna of the radar are deemed to be parallel since the target source is located in the "far field" of the radar, i.e., the distance between them is larger than $2A^2/\lambda$, where A is the diameter of the radar's antenna array and λ is wavelength of the signal carrier. As long as the switching is sufficiently fast, the target source's direction will be found through the Doppler shift caused by the switching [39], [40].

More specifically, a Doppler shift imitated by the switching between two receive antennas (RAs) at a radar is $f_d = A\cos\psi/(T_s\lambda)$, where ψ is the target source's direction with respect to the line of RAs and T_s is the switching time [41], [42].

Inspired by this principle, we set the switching time at symbol level and vary the deployment of antennas at the transmitting UAV to cause the Doppler shift at receiving UAVs, which will activate effectual MIMO configurations by converting the non-invertible channel matrices due to dominated LoS path into invertible ones, within a UAV network. The flexible deployment of the TAs lies in the adjustments of the distances and the angles between the TAs, where a polar coordinate system is set by taking the location of a TA as the pole. The locations of the other TAs at the transmitting UAV are adjusted by modifying their radial and angular coordinates.

Moreover, the trajectories of UAVs are predetermined in a UAV network and, therefore, their relative locations are (semi-)deterministic. This practical scenario can be utilised to further improve the performance of pseudo-Doppler principle-based antenna deployment within UAV networks.
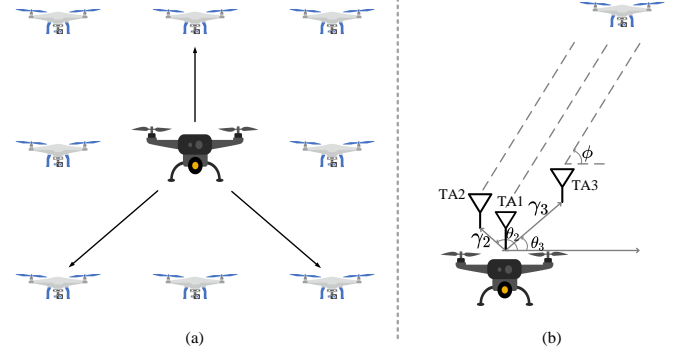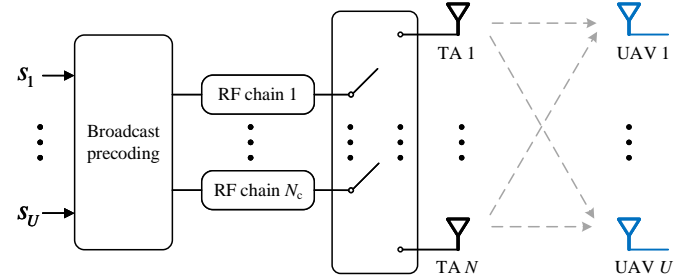

Fig. 2. A 1-to-U broadcast channel with N TAs and N_c RF chains at the broadcasting UAV.

B. Channel Model

Consider a UAV-to-UAV communication network that involves a predetermined group of UAVs, as shown in Fig. 1, where the multi-antenna UAVs transmit distinct data streams to several peer UAVs around them. Herein, a 1-to-3 UAV broadcast channel model is taken as an example, where the broadcasting UAV has 3 TAs and a polar coordinate system is formed. The location of TA 1 is set to the pole, whilst the locations of TA 2 and TA 3 are labelled by (γ_2, θ_2) and (γ_3, θ_3), respectively, where γ_n and θ_n are their radial and angular coordinates, $n \in \{2, 3\}$. The angular coordinate of a receiving UAV is denoted by ϕ.

Without loss of generality, a 1-to-U broadcast channel in this network is shown in Fig. 2, where a UAV having N TAs and N_c RF chains broadcasts U data streams to U single-antenna UAVs, $U \leqslant N$. This channel model can be generalised straightforwardly to the case with multi-antenna receivers by broadcasting N_r data streams, where N_r is the total number of all the receivers' antennas.

The flat-fading channel spanning from the broadcasting UAV to the receiving UAVs is modelled by a $U \times N$ Rician matrix with a deterministic LoS path, as [43], [44]

$$\mathbf{H} = \sqrt{\frac{K}{K+1}}\mathbf{D} + \sqrt{\frac{1}{K+1}}\tilde{\mathbf{H}}, \qquad (1)$$

where the $U \times N$ matrices $\mathbf{D}$ and $\tilde{\mathbf{H}}$ contain the deterministic components in the LoS path and the random components in the scattered paths, respectively. The $(u, n)^{\mathrm{th}}$ entry of $\mathbf{H}$ is

the channel coefficient from the nth TA at the broadcasting UAV to the uth receiving UAV. The $(u, n)^{\text{th}}$ entries of $\mathbf{D}$ and $\tilde{\mathbf{H}}$ are denoted by d_{un} and $\tilde{h}_{un}$, respectively, $u = 1, 2, \cdots, U$, $n = 1, 2, \cdots, N$, where d_{un} are constants and $\tilde{h}_{un}$ are independent and identically distributed (i.i.d.) complex Gaussian random variables with zero-mean and unit variance, i.e., $\tilde{h}_{un} \sim \mathcal{CN}(0, 1)$. The Rician factor K stands for the power ratio of $\mathbf{D}$ to $\tilde{\mathbf{H}}$.

Thus, the received signals at the U receiving UAVs are contained by a $U \times 1$ vector expressed as

$$\mathbf{y} = \mathbf{H}\mathbf{x} + \mathbf{z}, \tag{2}$$

where $\mathbf{y} = [y_1, y_2, \cdots, y_U]^{\text{T}}$ with y_u denoting the received signal at the uth receiving UAV, $u = 1, 2, \cdots, U$. The $U \times 1$ vector $\mathbf{z} = [z_1, z_2, \cdots, z_U]^{\text{T}}$ is composed of the received additive white Gaussian noise (AWGN) components, where $z_u \sim \mathcal{CN}(0, \sigma_Z^2)$ is the AWGN component at the uth receiving UAV. In addition, the $N \times 1$ vector $\mathbf{x}$ contains the signals transmitted from the broadcasting UAV.

To achieve a better broadcast, the transmitted signals are generated through precoding, expressed as

$$\mathbf{x} = \mathbf{W}\mathbf{s}, \tag{3}$$

where the $N \times U$ matrix $\mathbf{W}$ is the broadcast precoding matrix and the $U \times 1$ vector $\mathbf{s} = [s_1, s_2, \cdots, s_U]^{\text{T}}$ contains the amplitude-phase modulation (APM) symbols to be conveyed towards the U receiving UAVs. If M-ary APM is adopted by the broadcasting UAV, the APM symbol to be conveyed towards the uth receiving UAV, $s_u \in \{\alpha_1, \alpha_2, \cdots, \alpha_M\}$, where α_m is the mth symbol in the M-ary APM, $m = 1, 2, \cdots, M$. There are $L = M^U$ combinations of APM symbols contained by $\mathbf{s}$.

As a result, the received signals in (2) can be rewritten as

$$\mathbf{y} = \mathbf{H}\mathbf{W}\mathbf{s} + \mathbf{z}. \tag{4}$$

III. JOINT PRECODING AND ARRAY DESIGN IN UAV BROADCAST CHANNELS

In this section, the general principle of our joint precoding and array design is proposed for broadcast in the Internet of UAVs.

The objective of our design is to further reduce the number of RF chains required in the broadcast. In previous works, the number of RF chains needed, N_c, is equal to the number of receivers or the number of data streams. As the number of receivers and the number of data streams are both equal to U in our work, we aim to have $N_c \leqslant U - 1$. Therefore, our design principle for the broadcast precoding matrix $\mathbf{W}$ is that at least one null entry is prescribed in the transmitted vector $\mathbf{x}$ for all L possible combinations of APM symbols contained by $\mathbf{s}$.

For the purpose of mitigating the strong inter-stream interference due to high LoS strength in the Internet of UAVs, the broadcast precoding matrix $\mathbf{W}$ is formatted in terms of the LoS path $\mathbf{D}$, based on the zero-forcing concept, as

$$\mathbf{W} = \mathbf{D}^\dagger \left(\mathbf{D}\mathbf{D}^\dagger \right)^{-1}. \tag{5}$$

As such, the LoS path will be optimised through the pseudo-Doppler antenna array design at the broadcasting UAV to guarantee a full elimination of the LoS inter-stream interference, according to the locations of receiving UAVs.

To detail the pseudo-Doppler principle, we set up a polar coordinate system as shown in Fig. 1(b) and take the location of the broadcasting UAV's TA 1 as the pole. The locations of the other TAs at the broadcasting UAV are labelled by (γ_n, θ_n), where γ_n and θ_n are the radial and angular coordinates of the broadcasting UAV's TA n, respectively. The angular coordinate of the uth receiving UAV is denoted by ϕ_u. Given this polar coordinate system, the far-field LoS path in (1) is formed by the pseudo-Doppler principle [38], [40] as

$$\mathbf{D} = \begin{bmatrix} 1 & \exp\left(\dfrac{j2\pi\gamma_2\cos(\theta_2-\phi_1)}{\lambda}\right) & \cdots & \exp\left(\dfrac{j2\pi\gamma_N\cos(\theta_N-\phi_1)}{\lambda}\right) \\ \vdots & \vdots & \ddots & \vdots \\ 1 & \exp\left(\dfrac{j2\pi\gamma_2\cos(\theta_2-\phi_U)}{\lambda}\right) & \cdots & \exp\left(\dfrac{j2\pi\gamma_N\cos(\theta_N-\phi_U)}{\lambda}\right) \end{bmatrix}, \tag{6}$$

where λ is wavelength of the signal carrier.

Our design will make the LoS path in (6) match the broadcast precoding matrix in (5), through the antenna array design at the broadcasting UAV. The objective is to guarantee free inter-stream interference over the LoS path together with the RF chain reduction by leaving at least one null entry in the transmitted signals contained by $\mathbf{x}$.

IV. DESIGN PARADIGMS

In this section, the paradigms of 1-to-2 and 1-to-3 broadcasting are presented to further illustrate our joint design of broadcast precoding matrix and pseudo-Doppler antenna array in the Internet of UAVs. Herein, to make full use of the broadcasting UAV's TAs, we utilise the N TAs to serve N receiving UAVs, i.e., the number of receivers, $U = N$, and there are N distinct data streams over the broadcast channels. Moreover, unit-energy BPSK is adopted by the broadcasting UAV, i.e., the APM symbols in (3), $s_n \in \{1, -1\}$, $n = 1, 2, \cdots, N$.

A. 1-to-2 LoS Design

In this paradigm, we demonstrate the joint precoding and antenna array design in a 1-to-2 broadcast channel, i.e., $U = N = 2$, where the LoS path and the broadcast precoding matrix are represented by $\mathbf{D}^{(2)}$ and $\mathbf{W}^{(2)}$, respectively.

The transmitted signals at the broadcasting UAV can be denoted by a 2×1 vector $\mathbf{x}^{(2)} = \mathbf{W}^{(2)}\mathbf{s}^{(2)}$, where the 2×1 vector $\mathbf{s}^{(2)}$ contains the information-bearing BPSK symbols to be delivered towards the 2 receiving UAVs.

To ensure that only one TA is activated by the broadcasting UAV in an arbitrary transmission for the purpose of RF chain reduction, the precoding matrix $\mathbf{W}^{(2)}$ is designed to make $\mathbf{x}^{(2)}$ have one null entry and one non-zero entry, for all possible combinations of BPSK symbols consisting in $\mathbf{s}^{(2)}$ given by

$$\mathbf{S}^{(2)} = \begin{bmatrix} 1 & 1 & -1 & -1 \\ 1 & -1 & -1 & 1 \end{bmatrix} \triangleq \begin{bmatrix} \mathbf{s}_1^{(2)} & \mathbf{s}_2^{(2)} & -\mathbf{s}_1^{(2)} & -\mathbf{s}_2^{(2)} \end{bmatrix}. \tag{7}$$

Thanks to symmetry, the precoding matrix $\mathbf{W}^{(2)}$ designed according to the first two columns applies to the last two columns in a straightforward way. Therefore, we need to have one null entry and one non-zero entry in $\mathbf{W}^{(2)}\mathbf{s}_l^{(2)}$, $l = 1, 2$.

A general design of the precoding matrix in this case is denoted by

$$\mathbf{W}^{(2)} = \begin{bmatrix} \mu_1 & \mu_1 \\ \mu_2 & -\mu_2 \end{bmatrix} \triangleq \begin{bmatrix} \mathbf{w}_1^{(2)} \\ \mathbf{w}_2^{(2)} \end{bmatrix}, \quad (8)$$

where μ_1 and μ_2 are non-zero real numbers. With this design, we have $\mathbf{w}_1^{(2)}\mathbf{s}_2^{(2)} = 0$ when $\mathbf{s}_2^{(2)}$ is broadcast and $\mathbf{w}_2^{(2)}\mathbf{s}_1^{(2)} = 0$ when $\mathbf{s}_1^{(2)}$ is broadcast. As such, the broadcasting UAV always has a TA silent in an arbitrary transmission for any combination of two BPSK symbols to be broadcast. In other words, a single RF chain can support two individual data streams delivered at the broadcasting UAV.

Based on the zero-forcing precoding, the LoS path is expected to be obtained in the form of

$$\mathbf{D}^{(2)} = \left(\mathbf{W}^{(2)}\right)^{-1} = \begin{bmatrix} \dfrac{1}{2\mu_1} & \dfrac{1}{2\mu_2} \\ \dfrac{1}{2\mu_1} & -\dfrac{1}{2\mu_2} \end{bmatrix}. \quad (9)$$

Note that, the matrix $\mathbf{D}$ in (6) is a general model of the far-field propagation. However, with BPSK modulation, the signal propagation is not affected by the imaginary components. Therefore, the far-field LoS path via the antenna array design in the 1-to-2 BPSK broadcast channel is written in the form of a real matrix as

$$\mathbf{D}^{(2)} = \begin{bmatrix} 1 & \cos\left(\dfrac{2\pi\gamma_2\cos(\theta_2-\phi_1)}{\lambda}\right) \\ 1 & \cos\left(\dfrac{2\pi\gamma_2\cos(\theta_2-\phi_2)}{\lambda}\right) \end{bmatrix}, \quad (10)$$

where the broadcasting UAV's TA 1 and TA 2 are located at the pole and the point (γ_2, θ_2), respectively. The angular coordinates of the 2 receiving UAVs are ϕ_1, ϕ_2.

To align the LoS path in (10) with the expected form given by (9), the antenna array design at the broadcasting UAV is formulated as the problem

$$\mathcal{P}1: \quad \gamma_2\cos(\theta_2-\phi) \neq \pm\lambda/4, \ \forall\phi \in \{\phi_1, \phi_2\}; \quad (11a)$$
$$(2\pi\gamma_2/\lambda)|\cos(\theta_2-\phi_1) \pm \cos(\theta_2-\phi_2)| = \pi. \quad (11b)$$

Except for the case that $|\phi_1 - \phi_2| = 0 \cup \pi$, the solution to this problem is

$$\begin{cases} \theta_2 \neq (\phi_1 + \phi_2 + q\pi)/2, & q \in \{0, \pm 1, \pm 2\}; \\ \gamma_2 = (\lambda/2)/|\cos(\theta_2-\phi_1) \pm \cos(\theta_2-\phi_2)|. \end{cases} \quad (12)$$

Considering the energy efficiency, the LoS design is further optimised to minimise the broadcasting UAV's transmit power $P_B = \left\|\mathbf{W}^{(2)}\right\|_F$. This optimisation is equivalent to

$$\mathcal{P}2: \quad \max_{\theta_2} \cos\left(\dfrac{\pi\cos(\theta_2-\phi_1)}{|\cos(\theta_2-\phi_1) \pm \cos(\theta_2-\phi_2)|}\right) \quad (13)$$
$$s.t. \ \theta_2 \neq (\phi_1 + \phi_2 + q\pi)/2, \quad q \in \{0, \pm 1, \pm 2\}.$$

A solution to the problem $\mathcal{P}2$ is given by

$$\begin{cases} \theta_2 = \phi_1 + \pi/2; \\ \gamma_2 = (\lambda/2)/|\sin(\phi_1 - \phi_2)|. \end{cases} \quad (14)$$

This is the optimal antenna array design at the broadcasting UAV for a 1-to-2 broadcast channel, and this design leads to the broadcast precoding matrix

$$\mathbf{W}^{(2)} = \begin{bmatrix} 1/2 & 1/2 \\ 1/2 & -1/2 \end{bmatrix}. \quad (15)$$

B. 1-to-3 LoS Design

Herein, the joint precoding and antenna array design in a 1-to-3 broadcast channel ($U = N = 3$) is developed, where the LoS path and the broadcast precoding matrix are denoted by 3×3 matrices $\mathbf{D}^{(3)}$ and $\mathbf{W}^{(3)}$, respectively.

The transmitted signals at the broadcasting UAV are contained by a 3×1 vector $\mathbf{x}^{(3)} = \mathbf{W}^{(3)}\mathbf{s}^{(3)}$, where the 3×1 vector $\mathbf{s}^{(3)}$ contains the BPSK symbols to be conveyed to the 3 receiving UAVs.

Our goal of the precoding matrix $\mathbf{W}^{(3)}$ design is to leave at least one null entry in $\mathbf{x}^{(3)}$ for all possible combinations of BPSK symbols contained by $\mathbf{s}^{(3)}$. Obviously, there are $L = 8$ combinations given by

$$\begin{bmatrix} 1 & 1 & 1 & 1 & -1 & -1 & -1 & -1 \\ 1 & 1 & -1 & -1 & -1 & -1 & 1 & 1 \\ 1 & -1 & 1 & -1 & -1 & 1 & -1 & 1 \end{bmatrix}. \quad (16)$$

Due to symmetry, the first four columns are taken into account for the design of $\mathbf{W}^{(3)}$ and the resultant precoding will be fit for the last four columns as well.

The first four columns of (16) are denoted by

$$\mathbf{S}^{(3)} = \begin{bmatrix} 1 & 1 & 1 & 1 \\ 1 & 1 & -1 & -1 \\ 1 & -1 & 1 & -1 \end{bmatrix} \triangleq \begin{bmatrix} \mathbf{s}_1^{(3)} & \mathbf{s}_2^{(3)} & \mathbf{s}_3^{(3)} & \mathbf{s}_4^{(3)} \end{bmatrix}, \quad (17)$$

and the matrix of (16) can be rewritten as $\left[\mathbf{S}^{(3)}, -\mathbf{S}^{(3)}\right]$. Hence, we need to prescribe at least one null entry in the 3×1 vector $\mathbf{W}^{(3)}\mathbf{s}_l^{(3)}$, $l = 1, 2, 3, 4$.

A general instance of the precoding matrix design can be expressed as

$$\mathbf{W}^{(3)} = \begin{bmatrix} \nu_1 & \nu_1 & 0 \\ \nu_2 & -\nu_2 & 0 \\ \nu_3 & \nu_4 & \nu_5 \end{bmatrix} \triangleq \begin{bmatrix} \mathbf{w}_1^{(3)} \\ \mathbf{w}_2^{(3)} \\ \mathbf{w}_3^{(3)} \end{bmatrix}, \quad (18)$$

where ν_1, ν_2 and ν_5 are non-zero real numbers. This design lays the 1×3 vector $\mathbf{w}_1^{(3)}$ in the null space of the matrix $\left[\mathbf{s}_3^{(3)}, \mathbf{s}_4^{(3)}\right]$ and $\mathbf{w}_2^{(3)}$ in the null space of $\left[\mathbf{s}_1^{(3)}, \mathbf{s}_2^{(3)}\right]$, i.e., $\mathbf{w}_1^{(3)}\mathbf{s}_3^{(3)} = 0$, $\mathbf{w}_1^{(3)}\mathbf{s}_4^{(3)} = 0$, $\mathbf{w}_2^{(3)}\mathbf{s}_1^{(3)} = 0$, and $\mathbf{w}_2^{(3)}\mathbf{s}_2^{(3)} = 0$. As such, there is at least one null input to the broadcasting UAV's TAs for all 8 possible combinations of BPSK symbols.

As the LoS path is subsequently designed based on the zero-forcing precoding, namely $\mathbf{D}^{(3)} = \left(\mathbf{W}^{(3)}\right)^{-1}$, the precoding matrix has to be reversible. To ensure the reversibility of the precoding matrix $\mathbf{W}^{(3)}$ in (18), the vector $\mathbf{w}_3^{(3)}$ is not in

the space spanned by $\mathbf{w}_1^{(3)}$ and $\mathbf{w}_2^{(3)}$. Then, the LoS path is obtained by

$$\mathbf{D}^{(3)} = \left(\mathbf{W}^{(3)}\right)^{-1} = \begin{bmatrix} \dfrac{1}{2v_1} & \dfrac{1}{2v_2} & 0 \\[2mm] \dfrac{1}{2v_1} & -\dfrac{1}{2v_2} & 0 \\[2mm] -\dfrac{v_3+v_4}{2v_1v_5} & \dfrac{v_3-v_4}{2v_2v_5} & \dfrac{1}{v_5} \end{bmatrix}. \quad (19)$$

On the other hand, the far-field LoS path can be formulated in terms of the pseudo-Doppler expression (6) as

$$\mathbf{D}^{(3)} = \begin{bmatrix} 1 & \cos\left(\dfrac{2\pi\gamma_2\cos(\theta_2-\phi_1)}{\lambda}\right) & \cos\left(\dfrac{2\pi\gamma_3\cos(\theta_3-\phi_1)}{\lambda}\right) \\[2mm] 1 & \cos\left(\dfrac{2\pi\gamma_2\cos(\theta_2-\phi_2)}{\lambda}\right) & \cos\left(\dfrac{2\pi d_3\cos(\theta_3-\phi_2)}{\lambda}\right) \\[2mm] 1 & \cos\left(\dfrac{2\pi\gamma_2\cos(\theta_2-\phi_3)}{\lambda}\right) & \cos\left(\dfrac{2\pi\gamma_3\cos(\theta_3-\phi_3)}{\lambda}\right) \end{bmatrix}, \quad (20)$$

where the broadcasting UAV's TA 1 is located at the pole, and its TA 2 and TA 3 are labelled by (γ_2, θ_2) and (γ_3, θ_3), respectively. The angular coordinates of the 3 receiving UAVs are ϕ_1, ϕ_2, ϕ_3.

To match the LoS path in (20) to the condition given by (19), the antenna array design at the broadcasting UAV is formulated by the problem as

$$\mathcal{P}3: \quad \gamma_3\cos(\theta_3-\phi) = \pm\lambda/4, \ \forall\phi \in \{\phi_1, \phi_2\}; \quad (21a)$$
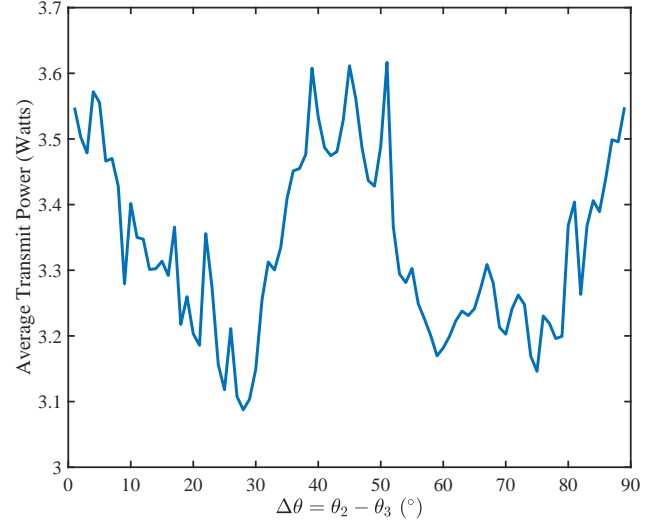
$$\gamma_3\cos(\theta_3-\phi_3) \neq \pm\lambda/4; \quad (21b)$$

$$\gamma_2\cos(\theta_2-\phi) \neq \pm\lambda/4, \ \forall\phi \in \{\phi_1, \phi_2\}; \quad (21c)$$

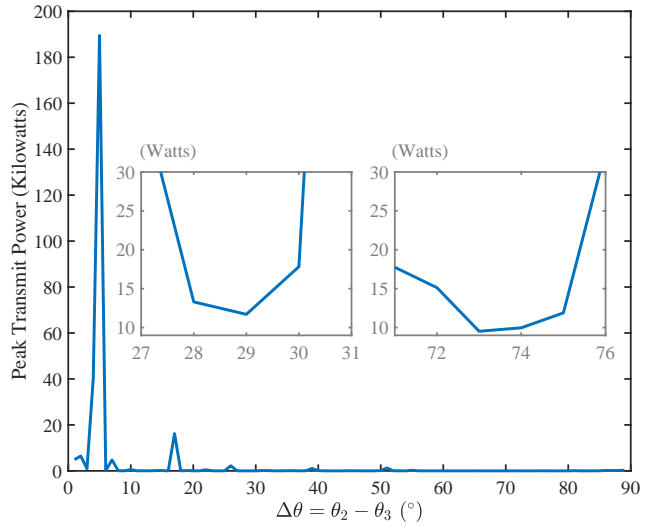$$(2\pi\gamma_2/\lambda)|\cos(\theta_2-\phi_1) \pm \cos(\theta_2-\phi_2)| = \pi. \quad (21d)$$

Note that there is no solution to this problem when $|\phi_1 - \phi_2| = 0 \cup \pi$, $|\phi_1 - \phi_3| = 0 \cup \pi$, or $|\phi_2 - \phi_3| = 0 \cup \pi$. Otherwise, the solution to this problem is given by

$$\begin{cases} \theta_3 = (\phi_1 + \phi_2 + p\pi)/2, & p \in \{0, \pm1, \pm2\}; \\ \gamma_3 = (\lambda/4)/|\cos(\theta_3-\phi_1)|; \\ \theta_2 \neq (\phi_1 + \phi_2 + q\pi)/2, & q \in \{0, \pm1, \pm2\}; \\ \gamma_2 = (\lambda/2)/|\cos(\theta_2-\phi_1) \pm \cos(\theta_2-\phi_2)|. \end{cases} \quad (22)$$

Once the locations of receiving UAVs are changing relative to the pole, the broadcasting UAV needs to redistribute its TA 2 and TA 3. In practice, the angular difference between θ_2 and θ_3 can be maintained constant and denoted by $\Delta\theta \triangleq \theta_2 - \theta_3$. To study the impact of this angular difference $\Delta\theta$ on the broadcasting UAV's transmit power, we investigate 10^6 random channel realizations for each fixed $\Delta\theta$, where the 3 receiving UAVs are located at random and the angular difference between any of them, $|\phi_u - \phi_{u'}| \geqslant \pi/12$, $u, u' = 1, 2, 3$, $u \neq u'$. Given that the transmit power of a BPSK symbol is deemed to be a benchmark for the unit power, namely 1 watt, the average transmit power and the peak transmit power of the broadcasting UAV, versus $\Delta\theta$, are compared in Fig. 3, where the signal carrier frequency is set to 3GHz in the UAV-enabled networking under study, i.e., the wavelength $\lambda = 0.1$ metres, and the angular difference $\Delta\theta = \theta_2 - \theta_3$ ranges from 0 to $\pi/2$. As shown in Fig. 3(a), the average transmit power achieves the minimum value at $\Delta\theta = 29°$. As shown in Fig. 3(b), the peak transmit power at $\Delta\theta = 29°$ is one of the lowest values.

(a) Average Transmit Power

(b) Peak Transmit Power

Fig. 3. The impact of the angular difference $\Delta\theta = \theta_2 - \theta_3$ on the broadcasting UAV's transmit power.

Therefore, taken into account the balance between the average transmit power and peak transmit power, $\Delta\theta = 29°$ is the best option for the angular difference between TA 2 and TA 3 at the broadcasting UAV.

This finding will facilitate our design in the 1-to-3 broadcasting. By setting the angular difference $\Delta\theta = 29°$, the solution to θ_2 in (22) is simplified as

$$\theta_2 = \theta_3 + \frac{29}{180}\pi. \quad (23)$$

Furthermore, to minimise the broadcasting UAV's transmit power P_B, the solution pertaining to the minimum of $\left\|\mathbf{W}^{(3)}\right\|_F$ among all feasible solutions is taken as the final solution of the optimal antenna array design at the broadcasting UAV. In detail, Algorithm 1 is developed to achieve the optimal antenna array design (γ_2, θ_2), (γ_3, θ_3) and the precoding matrix $\mathbf{W}^{(3)}$. Given the angular coordinates of the receiving

Algorithm 1 TA Distribution and Precoding Matrix

Input:

The angular coordinates of receiving UAVs, $\{\phi_1, \phi_2, \phi_3\}$;
The difference between θ_2 and θ_3, $\Delta\theta = 29°$.

Output:

The coordinates of broadcasting UAV's TA 2 and TA 3, (γ_2, θ_2) and (γ_3, θ_3).

1: $P_B = 0$;
2: **for** $\theta_3 = \{(\phi_1 + \phi_2)/2, \ (\phi_1 + \phi_2 + \pi)/2\}$ **do**
3:     $\gamma_3 = (\lambda/4)/|\cos(\theta_3 - \phi_1)|$;
4:     $\theta_2 = \theta_3 + \Delta\theta$;
5:     **for** $\gamma_2 = (\lambda/2)/|\cos(\theta_2 - \phi_1) \pm \cos(\theta_2 - \phi_2)|$ **do**
6:       Calculate the LoS path $\mathbf{D}^{(3)}$ in terms of (20);
7:       The precoding matrix $\mathbf{W}^{(3)} = (\mathbf{D}^{(3)})^{-1}$;
8:       **if** $P_B = 0$ or $P_B > \|\mathbf{W}^{(3)}\|_F^2$ **then**
9:         $P_B = \|\mathbf{W}^{(3)}\|_F^2$;
10:      **end if**
11:     **end for**
12: **end for**
13: Change the order of receiving UAVs and repeat the whole process.

UAVs, the optimal coordinates of the broadcasting UAV's TAs are obtained by searching among 4 possible solutions. In each search, the main operations include calculating the inverse and the Frobenius-norm of a 3-factorial square matrix, which is of low complexity for current computing devices. The algorithm returns the coordinates of TA 2 and TA 3 that minimise the broadcasting UAV's transmit power, which is always convergent.

V. PERFORMANCE ANALYSIS

In this section, the sum data rate and the BER of the multi-antenna UAV broadcast with our joint precoding and LoS design are formulated, based on which the performance of the proposed design is evaluated for the 1-to-2 and 1-to-3 broadcasting, with the wavelength of signal carrier, $\lambda = 0.1$ metres.

A. Metrics

In a 1-to-N UAV broadcast channel, the received signals over the Rician channel modelled in (1) are obtained by

$$\mathbf{y} = \left(\sqrt{\frac{K}{K+1}}\mathbf{D} + \sqrt{\frac{1}{K+1}}\tilde{\mathbf{H}}\right)\mathbf{W}\mathbf{s} + \mathbf{z}. \qquad (24)$$

As the broadcast precoding matrix is designed on the basis of the dominant LoS path, we have $\mathbf{DWs} = \mathbf{s}$ and, thus, the received signals can be rewritten as

$$\mathbf{y} = \sqrt{\frac{K}{K+1}}\mathbf{s} + \sqrt{\frac{1}{K+1}}\tilde{\mathbf{H}}\mathbf{W}\mathbf{s} + \mathbf{z}. \qquad (25)$$

Thereby, the LoS path is fully freed from the inter-stream interference, and the interference to a desired signal is from the scattered paths $\tilde{\mathbf{H}}$. Since BPSK modulation is adopted by the broadcasting UAV, all possible combinations of N BPSK

symbols contained by $\mathbf{s}$ are denoted by $\{\mathbf{s}_1, \mathbf{s}_2, \cdots, \mathbf{s}_L\}$, where $L = 2^N$. When the lth combination $\mathbf{s}_l$ is broadcast, the signal-to-interference-plus-noise power ratio (SINR) is obtained by

$$\rho_l = \frac{K}{(K+1)\sigma_Z^2 + \|\mathbf{W}\mathbf{s}_l\|_F^2}, \quad l = 1, 2, \cdots, L. \qquad (26)$$

1) Sum Data Rate: As the scattered paths contained by $\tilde{\mathbf{H}}$ are i.i.d., the sum data rate of the 1-to-N UAV broadcast channel with our joint precoding and antenna array design can be expressed as

$$R_{\text{sum}} = \frac{N}{L}\sum_{l=1}^{L} J\left(\sqrt{8\rho_l}\right), \qquad (27)$$

where $J\left(\sqrt{8\rho_l}\right)$ is the achievable data rate of a BPSK system at the SINR ρ_l, and the function $J(\eta)$ is detailed in [45] as

$$J(\eta) = 1 - \int_{-\infty}^{+\infty} \frac{e^{-(\xi - \eta^2/2)^2/(2\eta^2)}}{\sqrt{2\pi}\eta} \log_2\left(1 + e^{-\xi}\right) d\xi \qquad (28)$$

with $\lim_{\eta \to 0} J(\eta) = 0$ and $\lim_{\eta \to \infty} J(\eta) = 1$, $\eta > 0$.

2) Bit Error Rate: As BPSK symbols are delivered, the SINR per symbol, ρ_l, equals the SINR per bit and, accordingly, the BER of the 1-to-N UAV broadcast with our joint precoding and antenna array design is formulated as

$$\begin{aligned} \epsilon_b &= \frac{1}{L}\sum_{l=1}^{L} Q\left(\sqrt{2\rho_l}\right) \\ &= \frac{1}{L}\sum_{l=1}^{L} Q\left(\sqrt{\frac{2K}{(K+1)\sigma_Z^2 + \|\mathbf{W}\mathbf{s}_l\|_F^2}}\right), \end{aligned} \qquad (29)$$

where the Q-function is $Q(x) = (1/\sqrt{2\pi})\int_x^\infty \exp(-u^2/2)\mathrm{d}u$.

B. 1-to-2 Broadcast

The scenario in Fig. 4 is used to investigate a 1-to-2 broadcast case using our joint precoding and antenna array design, where the broadcasting UAV's TA 1 is located at the pole, and the angular coordinates of the 2 receiving UAVs are $\phi_1 = \pi/2$ and $\phi_2 = 0$. Conforming to (14), the broadcasting UAV's TA 2 is set at the point $(\lambda/2, \pi)$. With this optimal antenna array design, we have

$$\left\|\mathbf{W}^{(2)}\mathbf{s}_l^{(2)}\right\|_F^2 = 1, \qquad \forall l = 1, 2, 3, 4, \qquad (30)$$

where $\mathbf{W}^{(2)}$ is given by (15), and the 4 possible combinations of BPSK symbols contained by the 2×1 vector $\mathbf{s}^{(2)}$ are given by (7).

Hence, the SINR given that $\mathbf{s}_l^{(2)}$ is broadcast in this scenario is

$$\rho_l^{(2)} = \frac{K}{(K+1)\sigma_Z^2 + 1}, \qquad \forall l = 1, 2, 3, 4. \qquad (31)$$

The sum data rate in this case, i.e., $N = 2$, is achieved at

$$R_{\text{sum}}^{(2)} = 2J\left(\sqrt{\frac{8K}{(K+1)\sigma_Z^2 + 1}}\right), \qquad (32)$$

which is plotted in Fig. 5 versus the signal-to-noise power ratio (SNR) $1/\sigma_Z^2$. Since there are two individual data streams
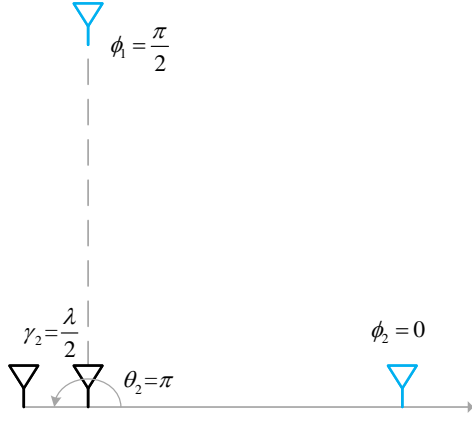
Fig. 4. A 1-to-2 broadcast case with the angular coordinates of receiving UAVs, $\phi_1 = \pi/2$ and $\phi_2 = 0$.
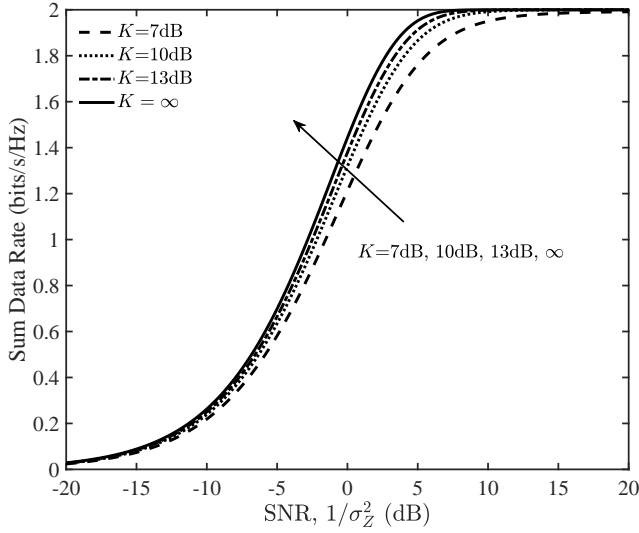

Fig. 5. Sum data rate achieved by the 1-to-2 broadcast case in Fig. 4.

of BPSK symbols delivered at the broadcasting UAV, the sum data rate converges to 2 bits/s/Hz as the SNR increases. Moreover, this broadcast channel achieves higher sum data rate as the Rician factor K increases.

The BER of this 1-to-2 broadcasting is calculated using

$$\epsilon_b^{(2)} = Q\left(\sqrt{\frac{2K}{(K+1)\sigma_Z^2 + 1}}\right), \tag{33}$$

which is plotted in Fig. 6. The simulation results are also provided in this figure to verify the theoretical calculation. As is shown in this figure, the BER performance gets better with the increase in the Rician factor K, which coincides with the phenomenon of higher sum data rate achieved by larger K in Fig. 5. The main reason behind this is that all the inter-stream interference comes from the scattered paths $\tilde{\mathbf{H}}$ and, therefore, it decreases as K increases. When $K = \infty$, there is no inter-stream interference at all and our design achieves the ideal performance. The increase of SNR widens the gap between practical performance and the ideal performance, since higher
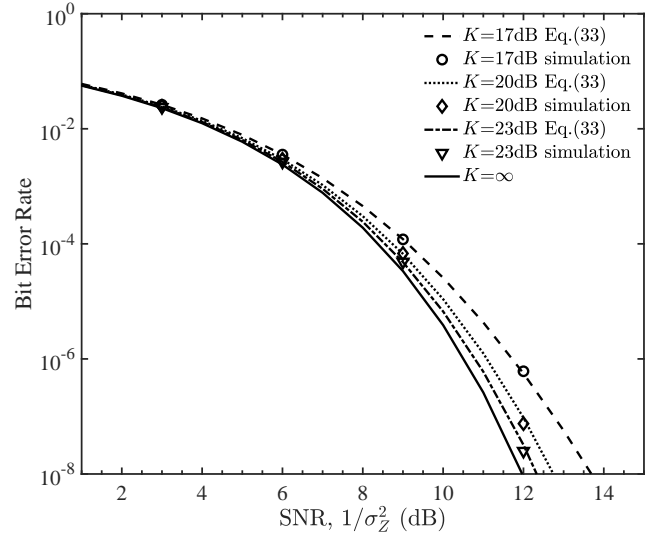

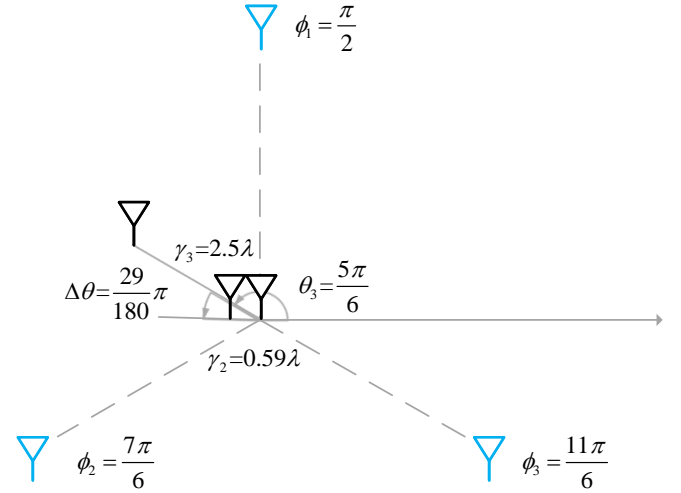Fig. 6. The BER performance of the 1-to-2 broadcast case in Fig. 4.

Fig. 7. A 1-to-3 broadcast case with the angular coordinates of receiving UAVs, $\phi_1 = \pi/2$, $\phi_2 = 7\pi/6$, $\phi_3 = 11\pi/6$, and the difference between the angular coordinates of the broadcasting UAV's TA 2 and TA 3, $\Delta\theta = 29°$.

SNR results in stronger inter-stream interference. However, the gap is negligible when $K \geqslant 20$dB. For example, at the BER of 10^{-8}, the performance gap between $K = 20$dB and $K = \infty$ is 0.7dB only.

C. 1-to-3 Broadcast

With the proposed joint precoding and antenna array design, the performance of a 1-to-3 broadcast case shown in Fig. 7 is investigated for $N = 3$, where the broadcasting UAV's TA 1 is located at the pole, and the angular coordinates of the 3 receiving UAVs are $\phi_1 = \pi/2$, $\phi_2 = 7\pi/6$, $\phi_3 = 11\pi/6$. According to the simplified solution (23), the difference between the angular coordinates of the broadcasting UAV's TA 2 and TA 3 is maintained constant, i.e., $\Delta\theta = \theta_2 - \theta_3 = 29°$.

Carrying out Algorithm 1, we obtain the optimal antenna array design of the broadcasting UAV's TA 2 and TA 3, i.e., at

the points $(179\pi/180, 0.59\lambda)$ and $(5\pi/6, 2.5\lambda)$, as well as the precoding matrix pertaining to the minimum transmit power, i.e.,

$$\mathbf{W}^{(3)} = \begin{bmatrix} 0.50 & 0.50 & 0.00 \\ 0.50 & -0.50 & 0.00 \\ 0.00 & 1.00 & -1.00 \end{bmatrix}. \tag{34}$$

Thus, we have all the possible broadcast signals as

$$\mathbf{W}^{(3)}\mathbf{S}^{(3)} = \begin{bmatrix} 1.00 & 1.00 & 0.00 & 0.00 \\ 0.00 & 0.00 & 1.00 & 1.00 \\ 0.00 & 2.00 & -2.00 & 0.00 \end{bmatrix}, \tag{35}$$

where $\mathbf{S}^{(3)}$ is given in (17). There are one or two null entries in each column of this matrix, which indicates that at most two RF chains are needed by the broadcasting UAV to support the delivery of three distinct data streams to individual UAVs. This design leads to the SINRs:

$$\rho_1^{(3)} = \rho_5^{(3)} = \frac{K}{(K+1)\sigma_Z^2 + 1}, \tag{36a}$$

$$\rho_2^{(3)} = \rho_6^{(3)} = \frac{K}{(K+1)\sigma_Z^2 + 5}, \tag{36b}$$

$$\rho_3^{(3)} = \rho_7^{(3)} = \frac{K}{(K+1)\sigma_Z^2 + 5}, \tag{36c}$$

$$\rho_4^{(3)} = \rho_8^{(3)} = \frac{K}{(K+1)\sigma_Z^2 + 1}. \tag{36d}$$

The sum data rate achieved by this 1-to-3 broadcasting is

$$R_{\text{sum}}^{(3)} = \frac{3}{8} \sum_{l=1}^{8} J\left(\sqrt{8\rho_l^{(3)}}\right), \tag{37}$$

which is plotted in Fig. 8 as a function of the SNR $1/\sigma_Z^2$. As is shown in this figure, the sum data rate converges to 3 bits/s/Hz with the increase in the SNR, due to three distinct data streams of BPSK symbols delivered at the broadcasting UAV. The same as the phenomenon found in Fig. 5, the 1-to-3 broadcast channel herein also achieves higher sum data rate as the Rician factor K increases.

The BER of this 1-to-3 broadcast design is obtained by

$$\epsilon_b^{(3)} = \frac{1}{4} \sum_{l=1}^{4} Q\left(\sqrt{2\rho_l^{(3)}}\right), \tag{38}$$

which is plotted in Fig. 9 versus the SNR $1/\sigma_Z^2$. The theoretical calculations are in good agreement with the simulation results. This figure reveals that the BER performance of our design gets better with the increase in the Rician factor K; the same phenomenon has been observed in Fig. 6. However, the performance gap between the practical case with $K \neq \infty$ and the ideal case with $K = \infty$ in the 1-to-3 broadcast channel is wider than that in the 1-to-2 broadcast channel, mainly because higher inter-stream interference is induced by more data streams.

VI. HIGHER-ORDER MODULATION

In this section, the paradigms discussed in Section IV are extended to the broadcast networks using M-ary APM ($M > 2$), where the modulated symbols are also broadcast
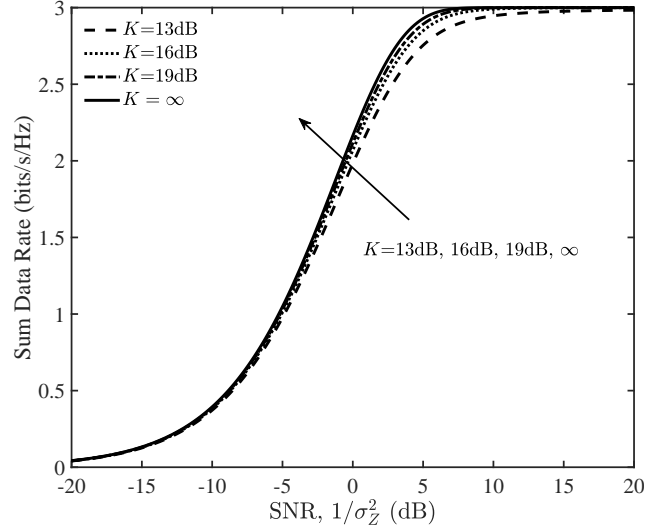

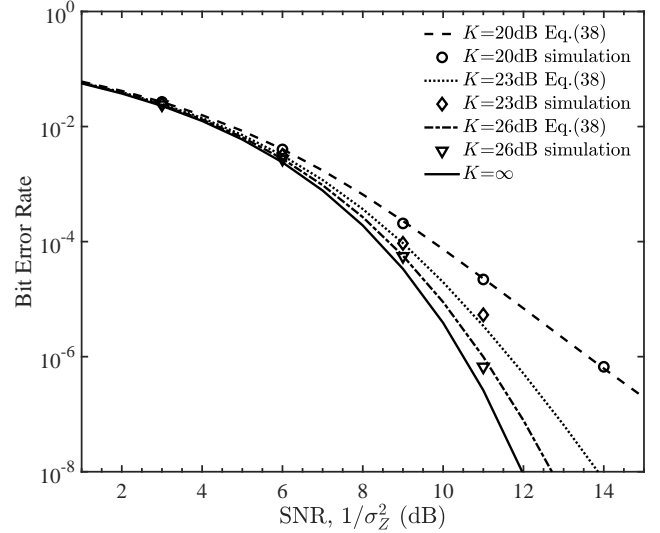Fig. 8. Sum data rate achieved by the 1-to-3 broadcast case in Fig. 7.

Fig. 9. The BER performance of the 1-to-3 broadcast case in Fig. 7.

to $U = N$ receiving UAVs through N distinct data streams. There are mainly two differences between the networks using M-ary APM ($M > 2$) and BPSK. Firstly, the M-ary APM ($M > 2$) symbols are distributed in the complex domain. Thus, the antenna array should be designed according to the complex form (6), rather than only taking the real part into consideration. Secondly, there are M^N possible combinations of the M-ary APM symbols to be transmitted. Not all the combinations can get a null entry in the transmission. Herein, the precoding matrix $\mathbf{W}$ is also formatted on the basis of the zero-forcing concept, i.e., $\mathbf{D} = \mathbf{W}^{-1}$, aiming to eliminate the inter-stream interference while implementing the RF chain reduction at the maximum probability.

A. 1-to-2 LoS Design

In this case, the 2×1 vector $\mathbf{s}^{(2)}$ containing two M-ary APM symbols s_1 and s_2 is delivered to 2 receiving UAVs, after

multiplied by the 2×2 precoding matrix $\mathbf{W}^{(2)}$. According to the difference between s_1 and s_2, the M^2 possible combinations of $\mathbf{s}^{(2)}$ can be reduced to M situations, denoted by $c_m = s_2/s_1$, $m = 1, \cdots, M$. A non-zero row vector in $\mathbf{W}^{(2)}$ generates a null entry for the transmission, given a value of c_m. In the 1-to-2 broadcast case, the RF chain can be reduced in the condition that $s_1 = s_2$ or $s_1 = -s_2$, i.e., $c_m = 1$ or -1. Therefore, the probability that the number of RF chains can be reduced is $2/M$.

The precoding matrix $\mathbf{W}^{(2)}$ is in the same form as (8), while its inverse is obtained by

$$\left(\mathbf{W}^{(2)}\right)^{-1} = \begin{bmatrix} \dfrac{1}{2\mu_1} & \dfrac{1}{2\mu_2} \\ \dfrac{1}{2\mu_1} & -\dfrac{1}{2\mu_2} \end{bmatrix} = \begin{bmatrix} 1 & \exp\left(\dfrac{j2\pi\gamma_2\cos(\theta_2-\phi_1)}{\lambda}\right) \\ 1 & \exp\left(\dfrac{j2\pi\gamma_2\cos(\theta_2-\phi_2)}{\lambda}\right) \end{bmatrix}. \quad (39)$$

The optimal solution to this equation group is the same as (14), and the resultant precoding matrix is the same as (15). That is, the antenna array design and the broadcast precoding matrix are both the same for any M-ary APM, $M \geqslant 2$, in the 1-to-2 broadcast case.

B. 1-to-3 LoS Design

In this case, a 3×1 vector $\mathbf{s}_l^{(3)}$ is to be precoded by the 3×3 matrix $\mathbf{W}^{(3)}$, where $l \in \{1, \cdots, M^3\}$ is the possible combination index of three M-ary APM symbols. If the $(n, u)^{th}$ entry of $\mathbf{W}^{(3)}$, denoted by $w_{n,u}$, is zero, the uth symbol s_u is not conveyed by TA n. In this way, the probability that TA n keeps silent can be improved. As $\mathbf{D}^{(3)} = \left(\mathbf{W}^{(3)}\right)^{-1}$ is in the form of (6) without any zero entry, there is at most one zero entry in each row or column in $\mathbf{W}^{(3)}$. Therefore, we formulate the precoding matrix in the 1-to-3 broadcast case as

$$\mathbf{W}^{(3)} = \begin{bmatrix} w_{1,1} & w_{1,2} & 0 \\ w_{2,1} & 0 & w_{2,3} \\ 0 & w_{3,2} & w_{3,3} \end{bmatrix}. \quad (40)$$

As shown in (6), the first column of $\left(\mathbf{W}^{(3)}\right)^{-1}$ is an all-ones vector, namely

$$\frac{-1}{w_{1,2}w_{2,1}w_{3,3} + w_{1,1}w_{2,3}w_{3,2}} \begin{bmatrix} -w_{2,3}w_{3,2} \\ -w_{2,1}w_{3,3} \\ w_{2,1}w_{3,2} \end{bmatrix} = \begin{bmatrix} 1 \\ 1 \\ 1 \end{bmatrix}. \quad (41)$$

The solution to (41) is given by

$$\begin{cases} w_{1,1} + w_{1,2} = 1; \\ w_{2,3} = -w_{2,1}; \\ w_{3,3} = -w_{3,2}. \end{cases} \quad (42)$$

Thus, a null input to TA 1 can be generated by the design of $w_{1,1}$ and $w_{1,2}$ in the condition that $s_1 = -s_2$, where we have $w_{1,1} = w_{1,2} = 1/2$. In this way, a general form of the precoding matrix is designed as

$$\mathbf{W}^{(3)} = \begin{bmatrix} 1/2 & 1/2 & 0 \\ w_{2,1} & 0 & -w_{2,1} \\ 0 & w_{3,2} & -w_{3,2} \end{bmatrix}, \quad (43)$$

and a null entry occurs if $s_1 = -s_2$, $s_2 = s_3$ or $s_1 = s_3$. In other words, the probability that the number of RF chains can be reduced is $3M(M-1)/M^3$.

Based on the zero-forcing precoding, the LoS path is rewritten as

$$\mathbf{D} = \left(\mathbf{W}^{(3)}\right)^{-1} = \begin{bmatrix} 1 & \dfrac{1}{2w_{2,1}} & -\dfrac{1}{2w_{3,2}} \\ 1 & -\dfrac{1}{2w_{2,1}} & \dfrac{1}{2w_{3,2}} \\ 1 & -\dfrac{1}{2w_{2,1}} & -\dfrac{1}{2w_{3,2}} \end{bmatrix}, \quad (44)$$

which is obtained through the antenna array design by solving the equation group

$\mathcal{P}4:$ $(2\pi\gamma_2/\lambda)\left[\cos(\theta_2-\phi_2) - \cos(\theta_2-\phi_1)\right] = \pi;$ (45a)

$(2\pi\gamma_2/\lambda)\left[\cos(\theta_2-\phi_3) - \cos(\theta_2-\phi_1)\right] = -\pi;$ (45b)

$(2\pi\gamma_3/\lambda)\left[\cos(\theta_3-\phi_2) - \cos(\theta_3-\phi_1)\right] = \pi;$ (45c)

$(2\pi\gamma_3/\lambda)\left[\cos(\theta_3-\phi_3) - \cos(\theta_3-\phi_1)\right] = 2\pi.$ (45d)

The solution to $\mathcal{P}4$ is given by

$$\begin{cases} \theta_2 = \arctan\left(\dfrac{\cos\phi_2 + \cos\phi_3 - 2\cos\phi_1}{2\sin\phi_1 - \sin\phi_2 - \sin\phi_3}\right); \\ \gamma_2 = \dfrac{\lambda/2}{\cos(\theta_2-\phi_2) - \cos(\theta_2-\phi_1)}; \\ \theta_3 = \arctan\left(\dfrac{\cos\phi_1 + \cos\phi_3 - 2\cos\phi_2}{2\sin\phi_2 - \sin\phi_1 - \sin\phi_3}\right); \\ \gamma_3 = \dfrac{\lambda/2}{\cos(\theta_3-\phi_2) - \cos(\theta_3-\phi_1)}. \end{cases} \quad (46)$$
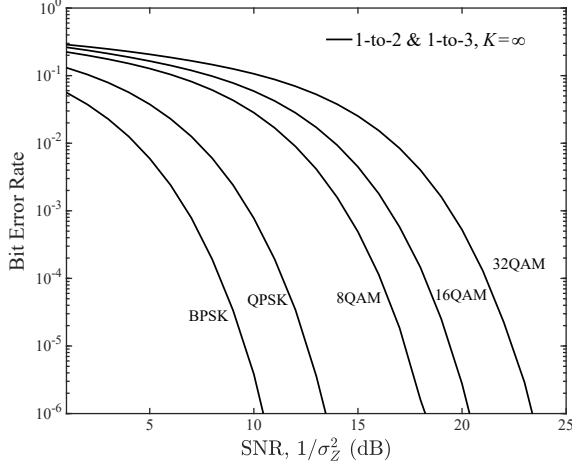
C. BER Performance

As shown in Sections VI-A and VI-B, our joint precoding and antenna array design can be extended to the broadcast cases with M-ary APM, $M > 2$, where the inter-stream interference is eliminated and the number of RF chains is reduced at a high probability. Fig. 10 illustrates the BER performance of the M-ary APM ($M \geqslant 2$) broadcast using the proposed design, where the UAV networking structures are shown in Fig. 4 and Fig. 7 for the 1-to-2 and 1-to-3 broadcast cases, respectively. In the 1-to-2 case, the broadcasting UAV's TA1 and TA2 are located at the pole and the point $(\lambda/2, \pi)$ respectively. The precoding matrix is

$$\mathbf{W}^{(2)} = \begin{bmatrix} 1/2 & 1/2 \\ 1/2 & -1/2 \end{bmatrix}. \quad (47)$$
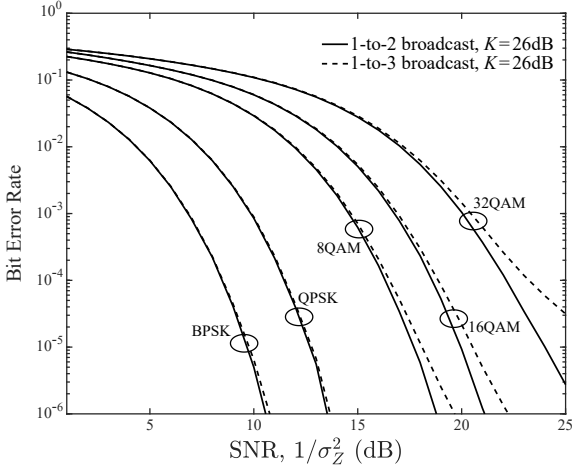
In the 1-to-3 case, TA 1, TA 2, and TA 3 are located at the pole, the point $(\lambda/\sqrt{3}, \pi)$ and the point $(\lambda/\sqrt{3}, -\pi/3)$, respectively. The precoding matrix is

$$\mathbf{W}^{(3)} = \begin{bmatrix} 1/2 & 1/2 & 0 \\ 1/2 & 0 & -1/2 \\ 0 & 1/2 & -1/2 \end{bmatrix}. \quad (48)$$

As shown in Fig. 10(a), the 1-to-2 and 1-to-3 broadcast cases achieve the same performance when $K = \infty$, because all the inter-stream interference has been eliminated in the LoS path. As shown in Fig. 10(b), with the increase in K, the scattered paths causes residual inter-stream interference, which results in the BER performance loss for both 1-to-2 and

(a) $K = \infty$

(b) $K = 26$dB

Fig. 10. The BER performance of 1-to-2 and 1-to-3 broadcast cases.

1-to-3 cases. Because a larger-scale antenna array undergoes higher inter-stream interference in the presence of scattered paths, the 1-to-2 broadcast achieves better BER performance than the 1-to-3 case, and the gap between them gets larger as the modulation-order M increases. Obviously, the broadcast with higher-order modulations is more sensitive to the residual inter-stream interference caused by scattered paths.

VII. DISCUSSIONS

A. Practicality

Herein, the main advantages of our joint precoding and array design are discussed from the perspective of its feasibility and validity in practice, as below.

1) Practical Channel Modelling: In the majority of theoretical studies on the Rician channel, the LoS path $\mathbf{D}$ is assumed to be an all-one matrix [44]. However, in practice, the far-field LoS path is embedded with the Doppler effect [43], which is determined by the relative position between the TA and RA, as shown in (6). Our joint precoding and array design is particularly proposed for this practical scenario.

2) Broadcast Precoding Design: The precoding matrix $\mathbf{W}$ in (3) is designed for two purposes: full elimination of the LoS inter-stream interference and RF chain reduction. For the first purpose, $\mathbf{W}$ is formed by (5), through adjusting the locations of TAs. For the second purpose, as many as zero entries are set in $\mathbf{Ws}$. Based on the design principle, the precoding matrices for 1-to-2 and 1-to-3 broadcasting have been provided, which can be extended to the broadcasting with more receiving UAVs, using the method similar with Algorithm 1. Moreover, the precoding matrix is designed for the scenario with a high Rician factor K. In the framework of Type-1 L-band Digital Aeronautical Communications System that offers data services under the LTE standards [49], K is up to 20dB, which is suitable for the application of our design.

3) Low Precoding Complexity: As the trajectories of UAVs are predetermined in a UAV network, the broadcasting UAV can prescribe the precoding matrix based on the (semi-)deterministic locations of the receiving UAVs, before constructing the network. As long as the relative positions between the broadcasting UAV and the receiving UAVs are not changed, the precoding matrix always works. Once the relative locations are varied, the broadcasting UAV needs to form a new precoding matrix.

4) High Spectral Efficiency: Relying on the Doppler effect, the far-field LoS path is exploited in the precoding design to eliminate the inter-stream interference for the multi-antenna broadcasting. In contrast to the single-antenna multiplexing schemes that rely on multiple frequency and/or time resource units in an orthogonal or non-orthogonal manner, our joint precoding and array design achieves much higher spectral efficiency by fully eliminating the LoS inter-stream interference in the multi-antenna broadcasting, for any order of modulation and any number of receiving UAVs, as shown in (5).

5) High Energy Efficiency: As shown in Section IV, our joint precoding and array design achieves full spatial multiplexing gain while ensuring that the number of active RF chains is 1 or 2 less than the number of data streams, using BPSK modulation. However, with the increase in the modulation order, the probability of the RF chain reduction is decreased, as investigated in Section VI.

B. Comparison with Spatial Modulation

As a prominent approach used for the RF chain reduction, SM conveys a portion of information through the selection of active TAs. Although the joint precoding and antenna array design is proposed for improving the QoS of multi-antenna broadcast in the Internet of UAVs with efficient RF chain reduction, it is different from the SM in the following aspects.

1) Application Scenario: SM relies on the independent fading channels in a multi-antenna system to distinguish different TAs, thus mapping a portion of information onto the TA indices. The spatial correlation between the fading channels degrades the SM performance [46], since the accuracy of the TA identification is lowered by the correlated channels. The original SM is not suitable for the UAV communications in LoS-dominated conditions, where the fading channels in a multi-antenna system are strongly correlated and become

unified as the LoS path gain increases. The phase rotations or amplitude variations have to be imposed on the symbols radiated from different TAs to distinguish the active one [47]. By contrast, the joint precoding and antenna array design is particularly conceived for the UAV communications in LoS-dominated conditions. Our current design is not suitable for the terrestrial communications in non-LoS conditions. Therefore, the combination of block-level or symbol-level precoding with our design are to be pursued for broader application scenarios, aiming to achieve better broadcasting QoS in ubiquitous wireless networks.

2) Design Principle: SM mainly aims at the improvement of achievable data rate through mapping a portion of information onto the active TA index, while requiring a single RF chain. The joint precoding and antenna array design mainly aims at the elimination of inter-stream interference in the Internet of UAVs, while reducing the number of RF chains.

3) Receiver Complexity: With SM in a multi-antenna system, the receiver needs to identify both the radiated symbol and the activated TA in a transmission. With the joint precoding and antenna array design in a multi-antenna UAV broadcast network, the detection at a receiving UAV is the same as that of the symbols received over an AWGN channel.

4) Channel information: SM needs accurate channel estimation to get fading channel coefficients in a multi-antenna system for the signal detection. The joint precoding and antenna array design needs a stable network structure, where the UAVs' relative locations are (semi-)deterministic. The loss of stability is equivalent to the introduction of extra inter-stream interference. To form a stable network structure for the Internet of UAVs, the hierarchical protocols, distributed gateway-selection algorithms and cloud-based stability-control mechanisms have been comprehensively reviewed in [48].

VIII. CONCLUSION

In the paper, a joint precoding and antenna array design was proposed, on the pseudo-Doppler basis, for the multi-antenna broadcast channels in the Internet of UAVs to reduce the number of RF chains while mitigating the inter-stream interference. With our proposed design, the broadcast precoding matrix was formatted to make at least one of the broadcasting UAV's TAs have null input in an arbitrary transmission, and the antenna array design was further exploited to fully eliminate the inter-stream interference over the LoS path. The joint design was actualised through the pseudo-Doppler effect at the broadcasting UAV. The algorithms with low computational complexity for optimising the antenna array design were developed to minimise the broadcasting UAV's transmit power in the paradigms of 1-to-2 and 1-to-3 broadcasting. Furthermore, the performance analysis in the metrics of sum data rate and BER substantiated the validity of our joint design, specifically in the UAV-enabled networking with high Rician factor.

In our joint precoding and antenna array design, the key to the RF chain reduction and the inter-stream interference elimination is the zero-forcing precoding. The precoding matrix formation and the deployment of TAs at the broadcasting UAV are determined by the far-field LoS path. As long as

the receiving UAVs are not very close to each other, the components of the LoS path can form a full-rank matrix. Thus, the algorithms and the paradigms presented in this work can be adapted to any topology changes with any number of receiving UAVs in a straightforward way.

The proposed design addresses precisely the major challenges in the Internet of UAVs. Firstly, the reduction of RF chains contributes the sanctification of the SWAP constraints on a multi-antenna UAV's broadcasting, which enables N_c RF chains to support the delivery of $N_c + 1$ or $N_c + 2$ distinct data streams. Secondly, the antenna array design at the broadcasting UAV eliminates the inter-stream interference over the LoS path, which is the dominant interference source in the UAV-enabled networking.

In LoS channels, i.e., $K = \infty$, the proposed design achieves the same performance as the signal passing through AWGN channels, where the performance loss at low SNRs can be compensated by improving the transmit power. As K decreases, the increased power gains of scattered paths results in extra inter-stream interference, which can be balanced by lowering the transmit power.

REFERENCES

[1] Y. Zeng, R. Zhang, and T. J. Lim, "Wireless communications with unmanned aerial vehicles: Opportunities and challenges", *IEEE Commun. Mag.*, vol. 54, no. 5, pp. 36-42, May 2016.

[2] X. Lin, *et al.*, "The sky is not the limit: LTE for unmanned aerial vehicles", *IEEE Commun. Mag.*, vol. 56, no. 4, pp. 204-210, Apr. 2018.

[3] O. S. Oubbati, N. Chaib, A. Lakas, P. Lorenz, and A. Rachedi, "UAV-assisted supporting services connectivity in urban VANETs", *IEEE Trans. Veh. Technol.*, vol. 68, no. 4, pp. 3944-3951, Apr. 2019.

[4] R. Duan, *et al.*, "Resource Allocation for Multi-UAV Aided IoT NOMA Uplink Transmission Systems", *IEEE Internet Things J.*, vol. 6, no. 4, pp. 7025-7037, Aug. 2019.

[5] J. Wang, *et al.*, "Multiple Unmanned-Aerial-Vehicles Deployment and User Pairing for Nonorthogonal Multiple Access Schemes", *IEEE Internet Things J.*, vol. 8, no. 3, pp. 1883-1895, Feb. 2021.

[6] J. Sun, *et al.*, "Aviation Data Lake: Using Side Information to Enhance Future Air-Ground Vehicle Networks", *IEEE Veh. Technol. Mag.*, vol. 16, no. 1, pp. 40-48, March 2021.

[7] L. Gupta, R. Jain, and G. Vaszkun, "Survey of important issues in UAV communication networks", *IEEE Commun. Surveys Tuts.*, vol. 18, no. 2, pp. 1123-1152, 2nd Quart., 2016.

[8] Y. Zeng, J. Lyu, and R. Zhang, "Cellular-connected UAV: Potential challenges and promising technologies", *IEEE Wireless Commun.*, vol. 26, no. 1, pp. 120-127, Feb. 2019.

[9] W. Mei, Q. Wu, and R. Zhang, "Cellular-connected UAV: Uplink association, power control and interference coordination", *IEEE Trans. Wireless Commun.*, vol. 18, no. 11, pp. 5380-5393.

[10] Y. Yang, "On the capacity of maximum selection in MIMO multicast network", in *Proc. IEEE INFOCOM Workshops*, Apr. 2008, pp. 1-5.

[11] Y. Yang and S. Aissa, "Common information multicast with different data rates", in *Proc. IEEE Veh. Technol. Conf. (VTC)*, Taipei, Jun. 2010, pp. 1-5.

[12] Y. Yang and S. Aissa, "On the capacity of multiple cognitive links through common relay under spectrum-sharing constraints", in *Proc. IEEE Int. Conf. Commun. (ICC)*, Kyoto, Jun. 2011, pp. 1-5.

[13] Y. Yang and S. Aissa, "On the coexistence of primary and secondary users in spectrum-sharing broadcast channels", in *Proc. IEEE Int. Conf. Commun. (ICC)*, Budapest, Jun. 2013, pp. 3085-3089.

[14] Y. Yang and S. Aissa, "Spectrum-sharing broadcast channels using fountain codes: Energy, delay and throughput", *IET Commun.*, vol. 8, no. 14, pp. 2574-2583, Aug. 2014.

[15] Y. Yang, K. Salama and S. Aissa, "Interference mitigation for broadcast in hierarchical cell structure networks: Transmission strategy and area spectral efficiency", *IEEE Trans. Veh. Technol.*, vol. 63, no. 8, pp. 3818-3828, Oct. 2014.

[16] Y. Yang, S. Aissa, A. Eltawil and K. Salama, "An interference cancellation strategy for broadcast in hierarchical cell structure", in *Proc. IEEE Global Commun. Conf. (GLOBECOM)*, Austin, Dec. 2014, pp. 1792-1797.

[17] M. Schubert and H. Boche, "Solution of the multiuser downlink beamforming problem with individual SINR constraints", *IEEE Trans. Veh. Technol.*, vol. 53, no. 1, pp. 18–28, Jan. 2004.

[18] Q. H. Spencer, A. L. Swindlehurst, and M. Haardt, "Zero-forcing methods for downlink spatial multiplexing in multiuser MIMO channels", *IEEE Trans. Signal Process.*, vol. 52, no. 2, pp. 461–471, Feb. 2004.

[19] T. Yoo and A. Goldsmith, "On the optimality of multiantenna broadcast scheduling using zero-forcing beamforming", *IEEE J. Sel. Areas Commun.*, vol. 24, no. 3, pp. 528-541, Mar. 2006.

[20] C. Masouros and E. Alsusa, "Dynamic linear precoding for the exploitation of known interference in MIMO broadcast systems", *IEEE Trans. Wireless Commun.*, vol. 8, no. 3, pp. 1396–1404, Mar. 2009.

[21] M. Alodeh, S. Chatzinotas, and B. Ottersten, "Constructive multiuser interference in symbol level precoding for the MISO downlink channel", *IEEE Trans. Signal Process.*, vol. 63, no. 9, pp. 2239–2253, May 2015.

[22] P. V. Amadori and C. Masouros, "Large scale antenna selection and precoding for interference exploitation", *IEEE Trans. Commun.*, vol. 65, no. 10, pp. 4529-4542, Oct. 2017.

[23] D. Persson, T. Eriksson, and E. G. Larsson, "Amplifier-aware multiple-input multiple-Output power allocation", *IEEE Commun. Lett.*, vol. 17, no. 6, pp. 1112-1115, Jun. 2013.

[24] S. K. Mohammed, "Impact of transceiver power consumption on the energy efficiency of zero-forcing detector in massive MIMO systems", *IEEE Trans. Commun.*, vol. 62, no. 11, pp. 3874-3890, Nov. 2014.

[25] Y. Yang and B. Jiao, "Information-guided channel-hopping for high data rate wireless communication", *IEEE Commun. Lett.*, vol. 12, no. 4, pp. 225-227, Apr. 2008.

[26] M. Di Renzo, H. Haas, and P. M. Grant, "Spatial modulation for multiple-antenna wireless systems: A survey", *IEEE Commun. Mag.*, vol. 49, no. 12, pp. 182–191, Dec. 2011.

[27] Y. Yang and S. Aissa, "Information guided channel hopping with an arbitrary number of transmit antennas", *IEEE Commun. Lett.*, vol. 16, no. 10, pp. 1552–1555, Oct. 2012.

[28] Y. Yang and S. Aissa, "Cross-layer combining of information-guided transmission with network coding relaying for multiuser cognitive radio systems", *IEEE Wireless Commun. Lett.*, vol. 2, no. 1, pp. 26-29, Feb. 2013.

[29] Y. Yang, "Spatial modulation exploited in non-reciprocal two-way relay channels: Efficient protocols and capacity analysis", *IEEE Trans. Commun.*, vol. 64, no. 7, pp. 2821–2834, Jul. 2016.

[30] X. Li, Y. Zhang, L. Xiao, X. Xu, and J. Wang, "A novel precoding scheme for downlink multi-user spatial modulation system", *Proc. IEEE Int. Symp. Pers. Indoor Mobile Radio Commun. (PIMRC)*, London, 2013, pp. 1361-1365.

[31] F. R. Castillo-Soria, J. Sanchez-Garcia, V. I. Rodriguez-Abdala, and R. Parra-Michel, "Multiuser MIMO downlink transmission using spatial modulation", in *Proc. IEEE Latin Amer. Conf. Commun. (LATINCOM)*, Cartagena de Indias, Colombia, Nov. 2014, pp. 1-5.

[32] M. A. Sedaghat, V. I. Barousis, R. R. Müller, and C. B. Papadias, "Load modulated arrays: A low-complexity antenna", *IEEE Commun. Mag.*, vol. 54, no. 3, pp. 46-52, Mar. 2016.

[33] S. Bhat and A. Chockalingam, "Detection of load-modulated multiuser MIMO signals", *IEEE Wireless Commun. Lett.*, vol. 7, no. 2, pp. 266-269, Apr. 2018.

[34] S. Hong and K. Oh, "Load-modulated single-RF MIMO transmission for spatially multiplexed QAM signals", in *Proc. IEEE Veh. Technol. Conf. (VTC)*, May 2015, pp. 1-6.

[35] O. El Ayach, S. Rajagopal, S. Abu-Surra, Z. Pi and R. W. Heath, "Spatially sparse precoding in millimeter wave MIMO systems", *IEEE Trans. Wireless Commun.*, vol. 13, no. 3, pp. 1499-1513, Mar. 2014.

[36] Z. Gao, L. Dai, D. Mi, Z. Wang, M. A. Imran, and M. Z. Shakir, "MmWave massive-MIMO-based wireless backhaul for the 5G ultra-dense network", *IEEE Wireless Commun.*, vol. 22, no. 5, pp. 13–21, Oct. 2015.

[37] R. W. Heath, N. González-Prelcic, S. Rangan, W. Roh, and A. M. Sayeed, "An overview of signal processing techniques for Millimeter wave MIMO systems", *IEEE J. Sel. Topics Signal Process.*, vol. 10, no. 3, pp. 436-453, Apr. 2016.

[38] D. N. Aloi and M. S. Sharawi, "Modeling and validation of a 915MHz single channel pseudo Doppler direction finding system for vehicle applications", in *Proc. IEEE Veh. Technol. Conf. (VTC)*, Sep. 2009, pp. 1-5.

[39] A. Gorcin and H. Arslan, "A two-antenna single RF front-end DOA estimation system for wireless communications signals", *IEEE Trans. Antennas Propag.*, vol. 62, no. 10, pp. 5321-5333, Oct. 2014.

[40] H. Won, *et al.*, "Developing a direction-finding system and channel sounder using a pseudo-Doppler antenna array", *IEEE Antennas Propag. Mag.*, vol. 61, no. 4, pp. 84-89, Aug. 2019.

[41] B. Jiao, "A quasi-Doppler method for doubling transmission efficiency through two orthogonal directions", arXiv:2007.07023 [eess.SP], Jul. 2020.

[42] D. Zheng and Y. Yang, "Pseudo-Doppler aided cancellation of self-interference in full-duplex communications", *Front. Sig. Proc.* 2:965551. doi: 10.3389/frsip.2022.965551.

[43] C. Tepedelenlioglu, A. Abdi, and G. B. Giannakis, "The Ricean K factor: Estimation and performance analysis", *IEEE Trans. Wireless Commun.*, vol. 2, no. 4, pp. 799-810, Jul. 2003.

[44] C. You and R. Zhang, "3D trajectory optimization in Rician fading for UAV-enabled data harvesting", *IEEE Trans. Wireless Commun.*, vol. 18, no. 6, pp. 3192-3207, Jun. 2019.

[45] S. ten Brink, "Convergence behavior of iteratively decoded parallel concatenated codes", *IEEE Trans. Commun.*, vol. 49, no. 10, pp. 1727-1737, Oct. 2001.

[46] Y. Yang and S. Aissa, "Information-guided communications in MIMO systems with channel state impairments", *Wirel. Commun. Mob. Comput.*, vol. 15, pp. 868-878, 2015.

[47] Y. Liu, Y. Yang, L. Yang, and L. Hanzo, "Physical layer security of spatially modulated sparse-code multiple access in aeronautical *ad-hoc* networking", *IEEE Trans. Veh. Technol.*, vol. 70, no. 3, pp. 2436–2447, 2021.

[48] J. Wang, *et al.*, "Taking Drones to the Next Level: Cooperative Distributed Unmanned-Aerial-Vehicular Networks for Small and Mini Drones", *IEEE Veh. Technol. Mag.*, vol. 12, no. 3, pp. 73-82, Sept. 2017.

[49] M. Sajatovic, *et al.*, "Updated LDACS1 system specification", *SESAR Joint Undertaking Report EWA04-1-T2-D1*, 2011.

Dongsheng Zheng received the B.E. degree in microelectronic science and engineering from the University of Electronic Science and Technology of China, Chengdu, China, in 2018. He is currently pursuing the Ph.D. degree in signal and information processing with the Department of Electronics, Peking University, Beijing, China. His research interests include ultra-reliable low-latency communications, signal processing in wireless communication and information theory.

Yuli Yang (Senior Member, IEEE) received the Ph.D. degree in Communications & Information Systems from Peking University, China, in July 2007. Her industry experience includes working with Huawei Technologies as an Intern Researcher from June 2006 to July 2007, and with Bell Labs Shanghai as a Research Scientist from August 2007 to December 2009. From January 2010 to December 2019, she was with King Abdullah University of Science & Technology, Melikşah University, and the University of Chester on various academic positions.

Since December 2019, she has been with the University of Lincoln as a Senior Lecturer in Electrical/Electronic Engineering. Her research interests include modelling, design, analysis and optimization of wireless systems and networks, specifically in physical-layer security, permutation-based modulation/transmission, ultra-reliable and low-latency communications.

Meng Ma received the B.S. and Ph.D. degrees in electrical engineering from Peking University, Beijing, China, in 2001 and 2007, respectively. From 2007 to 2011, he was an Assistant Professor with the School of Electronics, Peking University, where he has been an Associate Professor since 2011. From 2009 to 2010, he was a Visiting Scholar with Commonwealth Scientific and Industrial Research Organization, Sydney, Australia. His research interests include signal processing in wireless communication systems, interference cancellation technique, and information theory.

Wenyao Li received the B.E. degree in telecommunications engineering from Beijing University of Posts and Telecommunications, Beijing, China, in 2020. She is currently pursuing the Ph.D. degree in signal and information processing with the School of Electronics, Peking University, Beijing, China. Her research interests include ultra-reliable low-latency communications and signal processing in wireless communications.

Bingli Jiao (Senior Member, IEEE) received the B.S. and M.S. degrees from Peking University, China, in 1983 and 1988, respectively, and the Ph.D. degree from Saarland University, Germany, in 1995. He became an Associate Professor in 1995 and a Professor with Peking University in 2000. He currently is the director of Wireless Communication and Signal Processing Research Center, Peking University, Beijing, China. He is also a director of the Joint Laboratory for Advanced Communication Research between Peking University and Princeton University. His current research interests include full-duplex communications, information theory, and signal processing. He is a pioneer of co-frequency and co-time full-duplex as found in his early patent in 2006.